Photoinduced Electron Transfer in Dendritic Macromolecules. 1. Intermolecular Electron Transfer

ARTICLE *in* MACROMOLECULES · OCTOBER 1998

Impact Factor: 5.8 · DOI: 10.1021/ma980225i

3 AUTHORS, INCLUDING:

Chelladurai Devadoss
University of Illinois, Urbana-Champaign
26 PUBLICATIONS **3,063** CITATIONS

SEE PROFILE

Jeffrey S Moore
University of Illinois, Urbana-Champaign
427 PUBLICATIONS **27,021** CITATIONS

SEE PROFILE

Photoinduced Electron Transfer in Dendritic Macromolecules. 1. Intermolecular Electron Transfer

Chelladurai Devadoss,* P. Bharathi, and Jeffrey S. Moore*

Roger Adams Laboratory, Department of Chemistry, Materials Science & Engineering, and the Beckman Institute for Advanced Science and Technology, University of Illinois at Urbana−Champaign, Urbana, Illinois 61801

Received February 12, 1998; Revised Manuscript Received September 8, 1998

ABSTRACT: Photoinduced electron transfer in a series of dendritic macromolecules **1**−**6** has been investigated by a fluorescence quenching method. Both electron acceptors and electron donors quench the fluorescence of these dendrimers efficiently. The Stern−Volmer quenching constants for higher generation dendrimers for quenching by 1,4-diazabicyclo[2.2.2]octane (DABCO) are unusually large. Steady-state as well as time-resolved fluorescence spectroscopic studies indicate that there is a large contribution from static quenching in higher generation dendrimers. The evidence for ground-state complex formation has been obtained from a Benesi-Hildebrand plot for higher generation dendrimers and DABCO. Higher generation dendrimers also tend to form exciplexes with DABCO in tetrahydrofuran.

Introduction

Photoinduced electron transfer (PET) has been an active area of research because of its importance in biological photosynthesis as well as technical applications. Photoinduced charge transfer in the special pair of the reaction center is the primary step in a sequence of reactions in the photosynthesis process.[1] There are many current industrial applications that involve PET, and there is a growing list of potential applications in which PET plays a crucial role. For example, it finds applications in the initiation step of photopolymerization, photocuring, xerography, photovoltaics, photorefraction, and photocatalysis. In free radical photopolymerization the initiating radicals are generated by the PET from an amine to aromatic ketone.[2−4] Also, in some of the photoinitiated cationic polymerization involving onium salts, PET is the initial step after irradiation.[5] Similarly, PET plays a key role in the photocuring of resins and organic coatings.[4,6] It is well-known that in the conventional silver halide photography, electron transfer to Ag^+ ion to form metallic Ag after exposure is the primary step in the formation of the latent image.[7,8] It is also an important step in other forms of photoimaging and xerography which is based on photoconduction in a charged layer created by photoinduced generation of radical ion pairs.[9−11] Recently, Wasielewski et al. observed a high photorefractive gain in nematic liquid crystals doped with electron donor and acceptor molecules which undergo PET on irradiation.[12] A novel polymer with electron donor (carbazole) and electron acceptor (tricyanovinyl) groups that enhance the electrooptic effect for photorefractive applications has been reported by Peyghambarian and co-workers.[13] Of late, there has been a surge in the use of photocatalytic materials, mostly semiconductors, in the remediation of pollutants in wastewater and the environment. In all of these photocatalytic processes electron transfer is one of the critical steps.[14,15] Gratzel and co-workers reported the operation of photoelectrochemical cells for solar energy conversion where the important step is the PET from a dye to a semiconducting TiO_2 electrode.[16] Photocatalyzed oxidation of hydrocarbons in caged zeolites has been reported, and the initial step in this process is the PET from the hydrocarbon to O_2 to form the superoxide ion ($O_2^{-\bullet}$).[17] The importance of charge transfer (CT) complexes in polymeric devices and applications has also been well-documented.[18,19] Because of its importance and its ubiquitous nature in a variety of fields, PET has been intensively studied theoretically as well as experimentally. The results of various studies have been reviewed and discussed extensively.[20−24]

Recently, one class of molecules that has drawn considerable attention are the dendritic macromolecules or dendrimers for short.[25−28] They are characterized by a large number of terminal groups originating from a central focal point (core) having at least one branching at each repeat unit. An important feature of these highly symmetrical hyperbranched polymers is that they can be site-specifically functionalized. In our laboratory, using phenylacetylene (tolan) building blocks we have synthesized electroactive dendrimers to fabricate light-emitting diodes (LEDs) and photoactive dendritic macromolecules showing efficient light-harvesting antenna properties.[29,30] We report here our initial studies of PET in dendritic macromolecules with phenylacetylene repeat units. As a prelude to the study of intramolecular electron transfer in dendrimers with suitable functionality, intermolecular electron transfer has been carried out between dendrimers and electron donors/acceptors to gauge the feasibility of the process. Intermolecular electron-transfer involving dendrimers has also been reported by other groups on different dendritic systems. Turro et al. reported intermolecular electron transfer between tris(2,2′-bipyridine)ruthenium(II) [$Ru(bpy)_3^{2+}$] and methyl viologen MV^{2+} mediated through carboxylate-terminated dendrimers.[31] Even though the dendrimers did not take part directly in the electron-transfer reaction in this study, it provided a platform to bring together the donor [$Ru(bpy)_3^{2+}$] and acceptor MV^{2+} by adsorbing them at the terminal carboxylate groups. Such a close approach in homogeneous solution is unlikely due to electrostatic repulsion between the two positively charged reactants. Janssen

* To whom correspondence should be addressed.

10.1021/ma980225i CCC: $15.00
Published on Web 10/24/1998

Scheme 1. Phenyl-Terminated Dendrimers

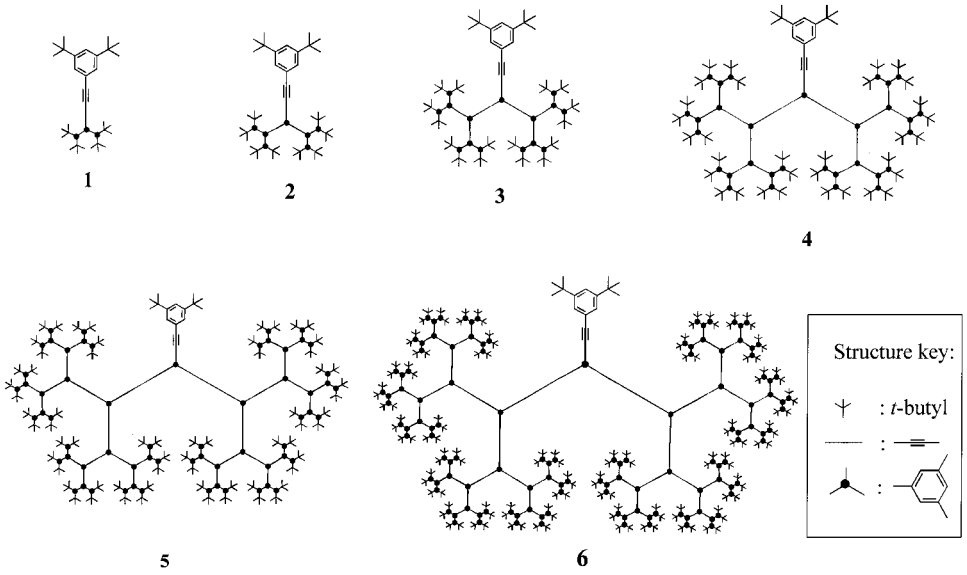

and co-workers studied the PET from functionalized dendrimers to C_{60} by observing the electron spin resonance (ESR) spectrum of $C_{60}^{-\bullet}$.[32] They concluded that the electron transfer depends on generation and higher generation dendrimers are better electron donors. A long-range PET between a carboxylate-terminated dendritic metallophorphyrin core and MV^{2+} which is adsorbed at the carboxylate groups has been described by Sadamoto and co-workers.[33] They used both steady-state and time-resolved fluorescence spectroscopy to examine the electron-transfer process. Intermolecular PET from dendritic zinc metallophthalocyanine to MV^{2+} through the dendritic architecture has been carried out by Kimura et al. using the method of fluorescence quenching.[34] From the very high values of the Stern−Volmer quenching constant (K_{SV}) in the latter two studies, it is inferred that the reactants have formed complexes in the ground-state itself and the reaction is not limited by diffusion of the reactants.

In this paper, we report the PET between a series of dendritic macromolecules **1**−**6** (Scheme 1) and an electron donor (DABCO). Initially, the simplest dendrimer, **1**, was chosen as the prototype for the series. The electron transfer was followed by the quenching of the fluorescence of the dendrimers using both steady-state and time-resolved fluorescence spectroscopy. Intermolecular electron transfer between **1** and electron donors (1,4-diazabicyclo[2.2.2]octane, DABCO and *p*-dimethoxybenzene, *p*-DMB) as well as acceptors (*p*-dicyanobenzene, *p*-DCB, and *meta*-dicyanobenzene, *m*-DCB) was studied. The electron transfer study was also carried out in solvents of different dielectric constants to elucidate the mechanism of the quenching process and subsequently to probe the effect of polarity on the rate constant. The fluorescence quenching was conducted with the whole series of dendrimers quenched by DABCO in tetrahydrofuran (THF) and acetonitrile/tetrahydrofuran (ACN/THF) mixed solvent systems. These two solvents were chosen as all of the six generations of dendrimers are soluble in these solvents. The nature of the quenching process, (i.e., dynamic or static) was analyzed, and the nature of intermediates in the electron transfer was also probed.

Experimental Section

(a) Materials. The synthesis, purification, and characterization of dendrimers (**1**−**6**) were described elsewhere.[30] These dendrimers were characterized by analytical techniques involving NMR, GPC, HPLC, mass spectrometry, and elemental analysis. The fluorescence quenchers, *p*-DCB, *m*-DCB, DABCO, and *p*-DMB, were purchased from Aldrich. DABCO was purified by recrystallization from a hexane/benzene mixed solvent followed by sublimation. All other quenchers were purified by recrystallization from aqueous ethanol. The solvents acetonitrile (ACN), cyclohexane (CHX), dichloromethane (DCM), and diethyl ether (DEE) were all spectroscopic grade and were used as purchased. The purity of the solvents was checked by recording the fluorescence spectrum of the neat solvent by exciting at 310 nm, the excitation wavelength used to study the fluorescence properties of the dendrimers.

(b) Spectroscopic Measurements. The UV−vis absorption spectra were recorded on a Shimadzu (model UV-160A) spectrophotometer using 1-cm quartz cells. Fluorescence spectra were recorded on a Photon Technology International (PTI) QM-1 fluorometer. The optical density of the solution for fluorescence measurements was less than 0.1 at the excitation wavelength. The fluorescence quantum yields of the samples were determined against quinine sulfate solution in 0.1 N H_2SO_4 ($\phi_{fl} = 0.55$) as the standard.[35] Fluorescence and excitation spectra were corrected for the wavelength dependence of detector sensitivity and excitation light source output. The spectra were recorded using a 1-cm quartz cuvette in the right angle geometry at room temperature.

Fluorescence lifetimes were measured on a time-correlated single photon counting fluorimeter (Edinburgh Instruments, model OB9000). The excitation source was a coaxial hydrogen flash lamp operated at 40 kHz. The emission was detected at a right angle to the excitation light with a Hamamatsu R955 photomultiplier tube (PMT) which was cooled to −22 °C. The response time of the PMT was 2.2 ns. A total of 10000 counts were collected at the maximum channel. The absorbance of the solutions was between 0.2 and 0.3 at the excitation wavelength. The fluorescence decay profile was analyzed by reconvolution of the instrumental response function and monoexponential or multiexponential decay of the emission using an iterative nonlinear least-squares curve-fitting method. The goodness of fit was assessed by using the plots of weighted residuals, reduced χ^2 values, and Durbin−Watson (DW) parameters.

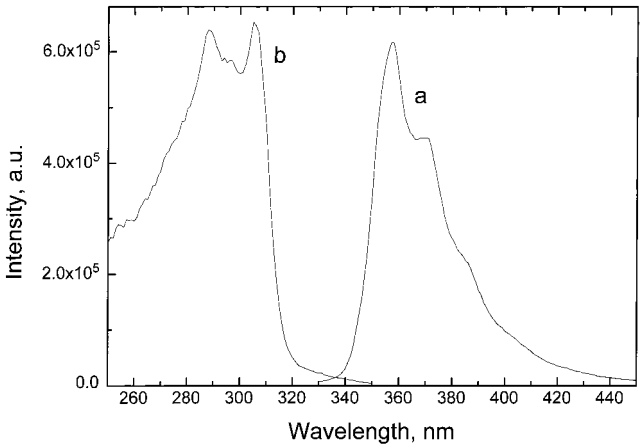

Figure 1. Fluorescence (a) and excitation (b) spectra of **1** in acetonitrile. The fluorescence spectrum was recorded by exciting at 310 nm and the excitation spectrum was recorded by monitoring at 370 nm.

Results

(a) Steady-State Spectral Properties of 1. The simplest of all the dendrimers in the series, **1** (see Scheme 1), was chosen as the model to study the fluorescence quenching by different electron acceptors and donors. The UV−vis absorption spectrum of **1** in ACN has the double peaks with maxima at 306.4 and 288.9 nm which are characteristic of dendrimers with phenylacetylene (tolan) repeat units.[36,37] The absorption spectrum is barely affected by the polarity of the solvent as the peak values are 308.2 and 290.4 nm in CHX. The corrected fluorescence and excitation spectra of **1** in ACN are shown in Figure 1. The emission spectrum recorded after excitation at 310 nm has maxima at 358 and 370 nm with a fwhm of 2087 cm^{-1}. Like the absorption spectrum, the position and the shape of the emission bands are insensitive to the polarity of the medium. The corrected excitation spectrum monitored at 370 nm exactly matches the absorption spectrum, and the fluorescence spectrum obtained with excitation at 290 nm is identical to that recorded with 310-nm excitation.

(b) Quenching of the Fluorescence of 1. When the fluorescence spectrum of **1** in ACN was recorded in the presence of added *p*-DCB, an electron acceptor, the fluorescence intensity was reduced. With increasing concentrations of *p*-DCB the quenching of the fluorescence also increased. Figure 2 shows the quenching of the fluorescence with increasing concentration of *p*-DCB. As the fluorescence becomes quenched, there is no concomitant new emission in the longer wavelength region which could arise due to the formation of an exciplex. The quenching of the steady-state fluorescence by an added quencher is analyzed using the Stern−Volmer equation (eq 1), where I_0 and I are the intensities of fluorescence in the absence and presence of the quencher respectively, K_{SV} is the Stern−Volmer quenching constant, and [Q] is the concentration of the quencher. As seen in eq 2, the K_{SV} is the product of τ_0, the lifetime of the fluorescing species in the absence of the quencher, and k_q the bimolecular quenching rate constant.

$$I_0/I = 1 + K_{SV}[Q] \quad (1)$$

$$K_{SV} = k_q\tau_0 \quad (2)$$

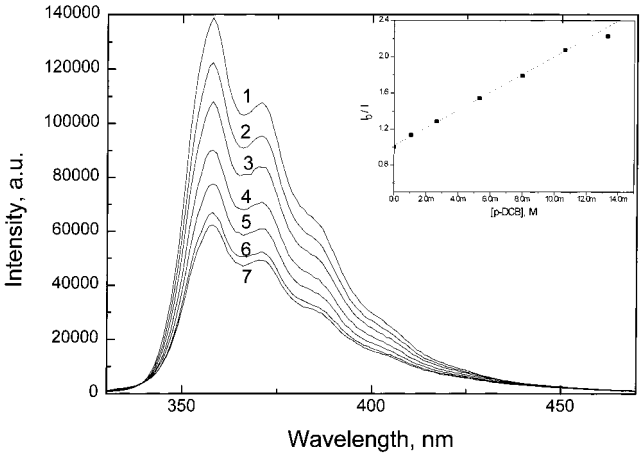

Figure 2. Quenching of the fluorescence of **1** in acetonitrile by different concentrations of p-DCB: (1) 0.0, (2) 1.07, (3) 2.67, (4) 5.33, (5) 8.0, (6) 10.66, and (7) 13.33 mM. The inset shows the Stern−Volmer plot for the fluorescence quenching.

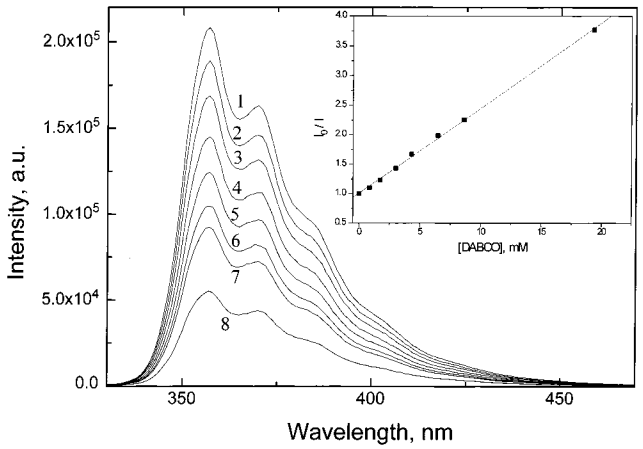

Figure 3. Quenching of the fluorescence of **1** in acetonitrile by different concentrations of DABCO: (1) 0.0, (2) 0.86, (3) 1.72, (4) 3.01, (5) 4.3, (6) 6.45, (7) 8.6, and (8) 19.35 mM. The inset shows the Stern−Volmer plot for the fluorescence quenching.

The inset in Figure 2 shows the Stern−Volmer plot for the fluorescence quenching. The Stern−Volmer quenching constant, K_{SV}, is 98.7 M^{-1}. Using a value of 9 ns for τ_0 (determined independently by the time-resolved fluorescence spectroscopy), the bimolecular quenching rate constant, k_q, was calculated to be 1.1×10^{10} M^{-1} s^{-1}. This value of k_q is of the order of the diffusion-controlled rate constant for ACN ($k_{diff} = 1.9 \times 10^{10}$ M^{-1} s^{-1}).[23] Subsequently, the fluorescence quenching was carried out with *m*-DCB, another electron acceptor with a lower reduction potential. The values of K_{SV} as well as k_q are lower by an order of magnitude than those observed for *p*-DCB. To make sure that the quenching of the fluorescence was not due to energy transfer from the excited state of **1** to the quencher, the absorption spectrum of the quencher was recorded and compared with that of **1**. For both quenchers used here, the spectrum of the quencher is blue-shifted from that of **1**, making the energy transfer a thermodynamically forbidden process.

The quenching of the fluorescence of **1** was continued with DABCO, an electron donor. The decrease in the fluorescence intensity with an increasing concentration of DABCO is shown in Figure 3. The inset shows the Stern−Volmer plot for the quenching process. The

Table 1. Rate Constants for the Quenching of the Fluorescence of 1 in Acetonitrile

quencher	redox potential, V[a]	K_{SV}, M^{-1} [b]	k_q, M^{-1} s^{-1}
p-DCB	−1.64	98.7	1.1×10^{10}
m-DCB	−1.79	10.8	1.2×10^{9}
DABCO	0.57	144	1.6×10^{10}
p-DMB	1.34	109	1.2×10^{10}

[a] The redox potential values were taken from ref 23. [b] Stern−Volmer quenching constants were determined from the steady-state fluorescence measurements.

Table 2. Rate Constants for the Quenching of the Fluorescence of 1 by DABCO in Different Solvents

solvent	dielectric constant, ϵ[a]	K_{SV}, M^{-1} [b]	k_q, M^{-1} s^{-1}
cyclohexane	2.02	55.4	3.4×10^{9}
tetrahydrofuran	7.58	93.3	6.0×10^{9}
ACN/THF (1:1)	24.6	105.5	6.9×10^{9}
acetonitrile	35.9	144	1.6×10^{10}

[a] The values of dielectric constants were taken from ref 46 and the value for ACN/THF was calculated from the molality and the known dielectric constants of each component. [b] Stern−Volmer quenching constants were determined from the steady-state fluorescence measurements.

quenching is very efficient and the value of K_{SV} is 144 M^{-1} which is greater than that observed for *p*-DCB. As in the case of *p*-DCB and *m*-DCB, there is no new emission band or spectral shift with an increasing amount of DABCO which discounts the formation of a complex between DABCO and excited **1**. When the quenching of the fluorescence was studied with another electron donor, *p*-DMB, efficient quenching was observed with a value of 109 M^{-1} for K_{SV}. The Stern−Volmer constant and quenching rate constants are collected in Table 1. The quenching rate constants correlate very well with the redox potentials of the quenchers. With the exception of *m*-DCB, the quenching rate constant is close to the diffusion-controlled reaction. Further, the fact that the quenching rate constant is large with both electron donors and acceptors indicates that dendritic macromolecule **1** is capable of accepting as well as donating electrons to suitable external quenchers in its excited singlet state.

To observe the effect of the nature of the solvent on the quenching process, a quenching study of **1** and DABCO was carried out in nonpolar CHX, mildly polar THF, and a polar THF/ACN (1:1) mixed solvent as well as in highly polar ACN. The quenching rate constants in these solvents are summarized in Table 2. With an increasing polarity of the medium, the quenching rate constant increases. This trend is expected for a quenching process that involves an electron transfer to the dendritic macromolecule from DABCO.

(C) Fluorescence Quenching as a Function of Generation. Having demonstrated that the fluorescence of **1** is quenched efficiently by electron donors, the quenching study was extended to the whole series of dendritic macromolecules (**1**−**6**) with DABCO. The structures of the six generations of dendritic macromolecules are shown in Scheme 1. Because of solubility limitations, the study was carried out in THF in which all the six generations are soluble. Figure 4 shows the UV−vis absorption spectra of 0.2 μM solutions of the dendrimers in THF. As expected, the absorption intensity, hence the extinction coefficient ϵ, increases with increasing generation. The inset shows the plot of log(ϵ) at the longer wavelength maximum as a function

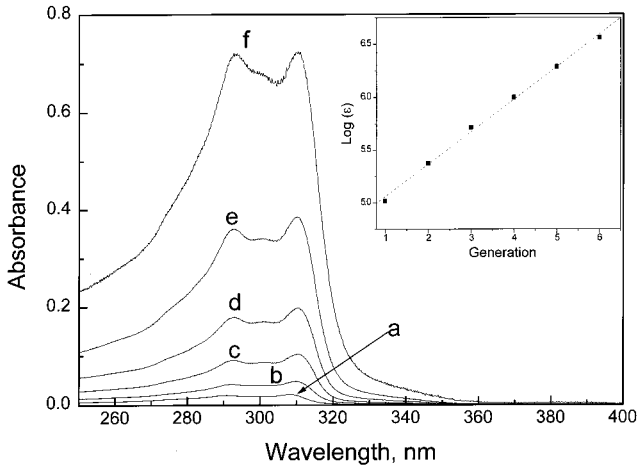

Figure 4. UV−vis absorption spectra of dendritic macromolecules **1**−**6** in tetrahydrofuran. (a) **1**, (b) **2**, (c) **3**, (d) **4**, (e) **5**, and (f) **6**. The spectra are normalized to a concentration of 0.2 μM. The inset shows the plot of log(ϵ) vs generation.

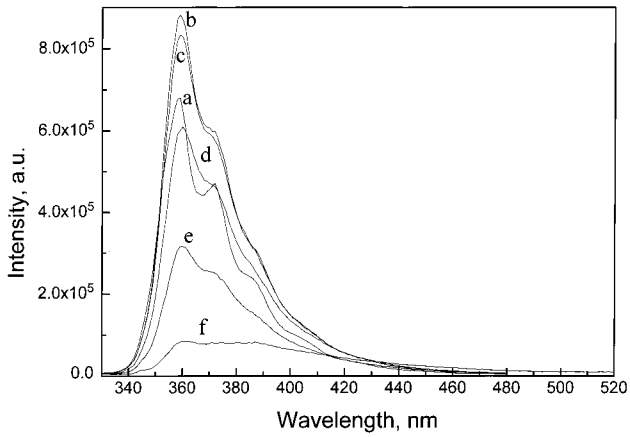

Figure 5. Fluorescence spectra of dendritic macromolecules **1**−**6** in tetrahydrofuran. (a) **1**, (b) **2**, (c) **3**, (d) **4**, (e) **5**, and (f) **6**. The spectra are normalized to a constant absorbance at the excitation wavelength, 310 nm.

of generation. As the number of phenylacetylene repeat units increases exponentially with the generation, there is a linear relationship between log(ϵ) and generation. A similar trend has been noticed for the same series of dendrimers in a dichloromethane solvent as reported earlier.[30] This observation and the lack of the generation-dependent spectral shift suggest that the electronic coupling between phenylacetylene repeat units is very weak in these dendrimers.

Figure 5 shows the fluorescence spectra of the six dendrimers in THF with excitation at 310 nm. The lower generation dendrimers have structural features which are absent in the higher generations. The absorption and fluorescence spectral parameters of the dendrimers are summarized in Table 3. Unlike the other dendrimers (**1**−**5**), the emission spectrum of **6** is very broad ($\Delta\nu_{1/2}$ = 4632 cm^{-1}) and has two maxima at 360 and 387 nm. Because of the large size of **6**, it can have access to different geometrical conformations which could result in broadening of the spectrum. The fluorescence quantum yield of higher generation dendrimers (**5** and **6**) are also low. The larger dendrimers may have many modes to dissipate the excitation energy which enhances the nonradiative decay. The Stoke's shift in all these dendrimers is around 4400 cm^{-1} which is moderate in magnitude and larger than expected for

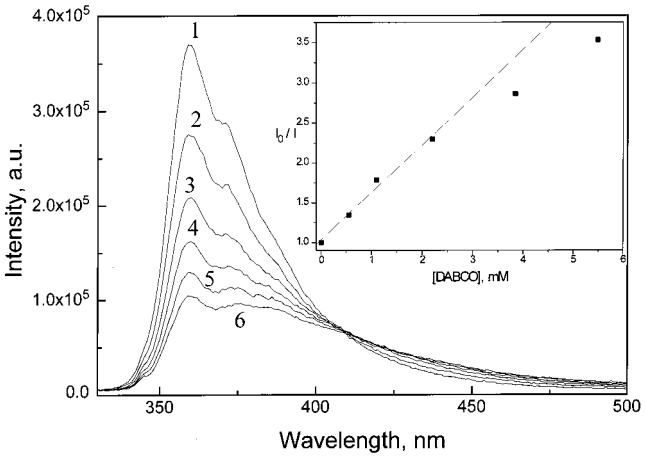

Figure 6. Quenching of the fluorescence of **1** in acetonitrile by different concentrations of DABCO: (1) 0.0, (2) 0.55, (3) 1.10, (4) 2.20, (5) 3.85, and (6) 5.50 mM. The inset shows the Stern−Volmer plot for the fluorescence quenching.

Table 3. Spectroscopic Parameters for 1−6 in Tetrahydrofuran

compound	λ_{max} (abs), nm	ϵ, M^{-1} cm^{-1}	λ_{max} (fl), nm	Stoke's shift, cm^{-1}	Φ_{fl}
1	308.2 290.8	1.04×10^5 9.55×10^4	359, 372	4591	0.27
2	309.6 292.0	2.37×10^5 2.10×10^5	359, 372	4445	0.34
3	310.2 292.8	5.19×10^5 4.56×10^5	359	4382	0.34
4	310.2 293.0	9.97×10^5 9.02×10^5	360	4459	0.28
5	310.2 292.8	1.94×10^6 1.77×10^6	360	4459	0.16
6	310.4 292.6	3.64×10^6 3.63×10^6	360, 387	4438	0.08

dendrimers made up of rigid aromatic hydrocarbon repeat units. This shift can be attributed to the relaxation of the solvent shell around the dendrimer rather to any structural relaxation.

The quenching of the fluorescence of **1** by DABCO in THF was very efficient with $K_{SV} = 93.3$ M^{-1} ($k_q = 5.9 \times 10^9$ M^{-1} s^{-1}). Similar quenching was observed for the other five dendrimers. However, two distinct differences between the behavior of lower generation dendrimers and higher generations are noted, especially for **5** and **6**. One feature is the extra emission in the longer wavelength region and the other is the nonlinear behavior of the Stern−Volmer plot. For instance, with an increasing amount of DABCO, the fluorescence of **5** is quenched strongly; simultaneously, there is an increase in the emission in the longer wavelength region (410−500 nm) as shown in Figure 6. The additional emission in the longer wavelength region may arise from an excited state−ground-state complex (exciplex) formed between the excited singlet state of **5** and DABCO. The absorption spectrum of **5** with added DABCO in the mM concentrations used in the fluorescence quenching study in THF does not show any spectral shift or new absorption band. The fluorescence from an exciplex is characterized by a broad structureless emission band which is dependent on the polarity of the medium. The emission spectrum of the exciplex was obtained by subtracting the emission spectrum of **5** without DABCO from that with DABCO after normalizing at 360 nm. Figure 7 shows the normalized

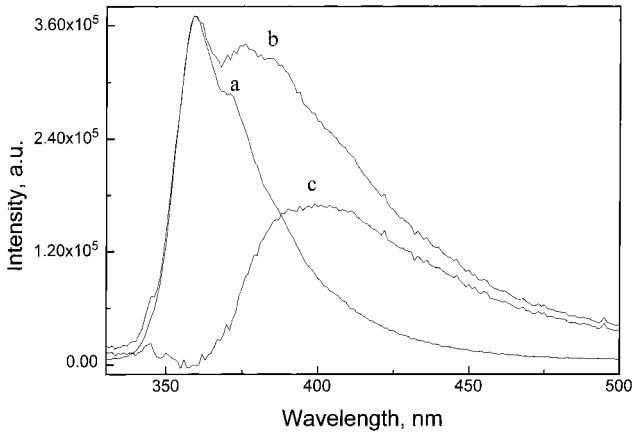

Figure 7. Fluorescence spectra of **5** in tetrahydrofuran (a) without DABCO, (b) with 5.5 mM DABCO, and (c) the difference of the normalized spectra (b − a).

spectra and the emission spectrum of the exciplex. The fluorescence maximum for the exciplex is at 399 nm in THF and 405 in an ACN/THF mixed solvent. To confirm the formation of exciplex between **5** and DABCO, the fluorescence decay of **5** with DABCO (7.95 mM) in THF was monitored at 360 and 400 nm. Figure 8 shows the decay traces monitored at these wavelengths. The decay profiles were fitted to triexponential function. The following values of the lifetimes were obtained.

emission	τ_1, ns	τ_2, ns	τ_3, ns
at 360 nm	5.25 (71.5%)	2.36 (21.4%)	0.38 (7.4%)
at 400 nm	5.9 (31.6%)	2.12 (46.1%)	0.41 (22.3%)

There is a vast difference in the contributions from different components at these two wavelengths. The decay monitored at 360 nm has major contribution from a longer-lived component whereas the one at 400 nm where the emission from the exciplex is predominant has larger contributions from short-lived components. Hence, the fluorescence at these two wavelengths come from different species. These results also indicate that the fluorescence lifetime of the exciplex is shorter than that of excited **5**.

Like **5**, **6** also displayed similar additional emission in the longer wavelength region with an increasing amount of DABCO. Separation of the emission due to exciplex gave a broad band with a maximum at 409 nm in THF and 480 nm in an ACN/THF mixed solvent. This red shift in the fluorescence with increasing polarity of the medium is clear evidence for the polar nature of the exciplex.

The inset in Figure 6 shows the Stern−Volmer plot for the quenching of the fluorescence of **5** by DABCO in THF. As can be seen from the inset, the plot is nonlinear with negative deviation. This suggests that the recorded intensity of the fluorescence is more than expected. This observation is additional evidence for the formation of exciplex in the system under study. The negative deviation occurs because of the overlap of the emission from the exciplex with the emission of **5**. In the case of **6**, the negative deviation was greater, indicating more intense fluorescence from the exciplex formed between the excited state of **6** and DABCO.

The Stern−Volmer quenching constant as a function of generation is shown in Figure 9. With increasing generation, K_{SV} increases up to that of **5** and then decreases. However, the values for higher generation

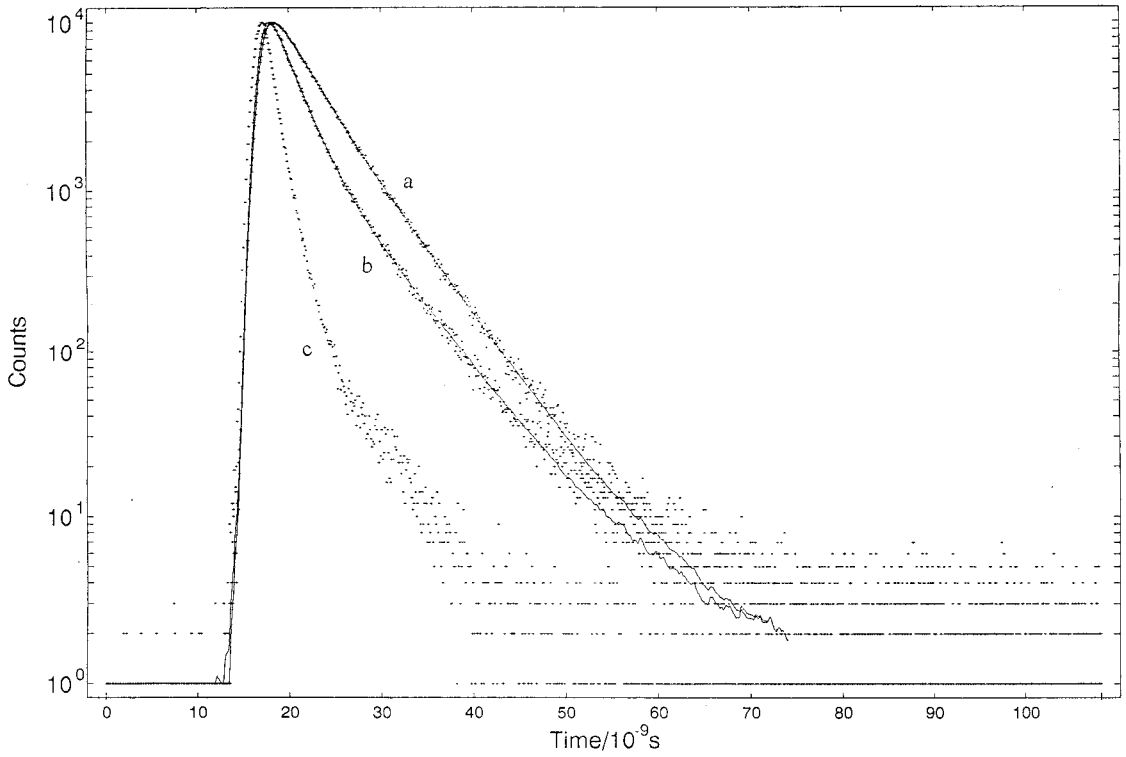

Figure 8. Fluorescence decay of **5** with 7.95 mM DABCO in THF measured by the single-photon counting method. (a) Monitored at 360 nm, (b) monitored at 400 nm, and (c) instrument response function (IRF).

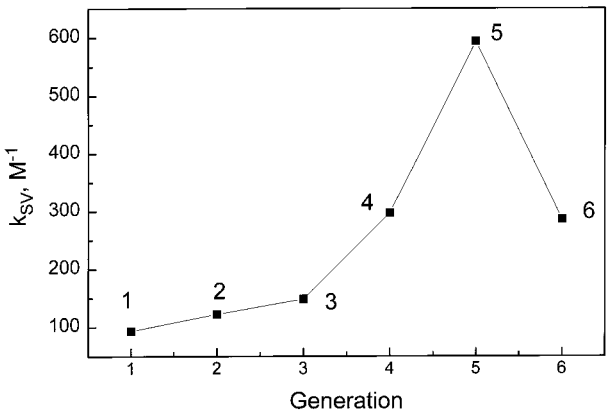

Figure 9. Stern−Volmer quenching constant as a function of generation. The quenching was carried out for the dendritic macromolecules **1**−**6** with DABCO in tetrahydrofuran. In the case of **5** and **6**, the slope (k_{SV}) was determined from the straight line drawn through the first few data points only because of high nonlinearity.

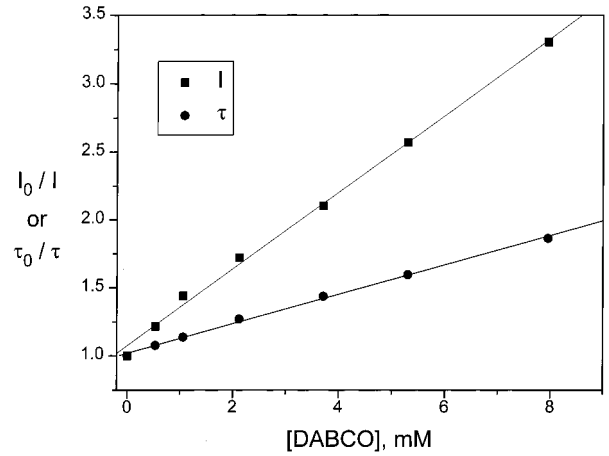

Figure 10. Stern−Volmer plots for the quenching of the fluorescence of **4** by DABCO in tetrahydrofuran. Data from the steady-state fluorescence intensity measurements (filled square) and from the lifetime measurements (filled circle).

dendrimers seem to be unusually high. It is possible that in higher generations static quenching might have contributed to the quenching process. To examine for the possibility of static quenching, the lifetimes of the excited dendrimers were recorded with various concentrations of DABCO. Similar to eq 1, the Stern−Volmer equation can be modified for lifetime measurements as given below:

$$\tau_0/\tau = 1 + K_{SV}[Q] \qquad (3)$$

where τ_0 and τ are the lifetimes of the dendrimer in the absence and presence of the quencher (DABCO), respectively. For **1**, the value of quenching constants obtained from steady-state quenching ($K_{SV}(I)$ = 93.3 M^{-1}) and that obtained from the fluorescence lifetime ($K_{SV}(\tau)$ = 101.0 M^{-1}) are equal within experimental error. Hence, in **1,** the quenching is exclusively due to a dynamic process. However, for the higher generation dendrimers (i.e., **4**, **5**, and **6)** the two values $K_{SV}(I)$ and $K_{SV}(\tau)$ differ significantly. For instance, Figure 10 shows the Stern−Volmer plots obtained from steady-state quenching and lifetime quenching measurements for **4**. The value of $K_{SV}(I)$ (287.2 M^{-1}) is larger than $K_{SV}(\tau)$ (111.5 M^{-1}), and this difference may be due to contribution from static quenching by DABCO. For **5**, the difference is much larger, suggesting larger contribution from static quenching for the fluorescence quenching process.

Discussion

First, the mechanism of the quenching of the fluorescence has to be elucidated. In general, the fluores-

Scheme 2

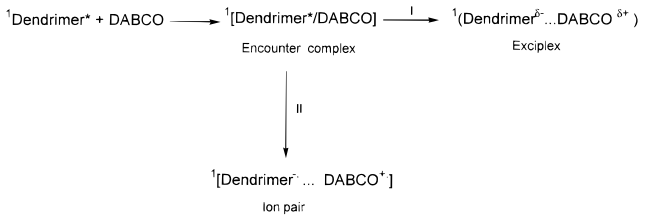

cence from an excited singlet state can be quenched by an added reagent by any one of the following processes: (i) energy transfer, (ii) electron transfer, and (iii) heavy-atom effect. Since the absorption spectra of the quenchers (*p*-DCB, *m*-DCB, DABCO, and *p*-DMB) are blue-shifted (higher energy) from that of the dendrimers, energy transfer from an excited dendrimer to the quencher is thermodynamically not favorable. Further, as the quenching rate constants are of the order of the diffusion-controlled rate constant, this facile quenching cannot be due to the thermodynamically unfavorable energy transfer. Normally, the presence of heavy atoms enhances intersystem crossing, leading to the formation of triplets and thus decreases the fluorescence. The absence of heavy atoms like Br and I in both the solvent and the reactants indicates that fluorescence quenching due to the heavy-atom effect can be ruled out. Hence, the fluorescence quenching can be ascribed to photoinduced electron transfer. This conclusion is corroborated by the correlation between redox potentials of the quencher and the quenching rate constant. Electron donors having a lower oxidation potential quench the fluorescence more effectively than one with a higher oxidation potential (DABCO vs *p*-DMB). Similarly, electron acceptors with higher reduction potential are stronger quenchers (*p*-DCB vs *m*-DCB). Additional evidence in support of an electron-transfer mechanism comes from the observation that the increasing polarity of the solvent increases the quenching rate constant which is a hallmark of electron transfer reactions. Calculations of free energy change for the electron-transfer based on the reported redox potential values for the tolan repeat unit, $E_{1/2}^{ox}$ of 1.85 V[38] and $E_{1/2}^{red}$ of −2.34 V,[39] clearly show that the electron-transfer reactions between the tolan units and the four fluorescence quenchers under study are exergonic. Hence, we can unequivocally conclude that electron transfer is the mechanism by which the fluorescence of the dendrimers are quenched upon the addition of redox-active donors or acceptors.

Second, the intermediate involved in the quenching process will be analyzed. In general, the formation of an exciplex is considered to be one of the intermediate steps in PET.[40−44] The exciplex is characterized by its broad structureless emission band at a longer wavelength than that of the fluorophore. In this study, in dendrimers **1**−**4**, additional emission in the longer wavelength region was not observed which indicates the absence of the formation of an emissive exciplex. Hence, in lower generation dendrimers, the intermolecular electron transfer occurs via the diffusion of the dendrimer and quencher to form the encounter complex which leads to the formation of ion pairs or to regenerate starting materials by back-electron transfer. In higher generation dendrimers, especially in **5** and **6**, additional emission in a longer wavelength region has been observed. Scheme 2 describes the quenching of the fluorescence of dendrimers.

It seems that the higher generation dendrimers follow route I whereas lower generation dendrimers follow route II. The exciplexes are polar in nature which can be evidenced by the bathochromic shift of the exciplex emission with an increasing polarity of the medium. For example, in **6** the fluorescence maximum for the exciplex in THF (dielectric constant $\epsilon = 7.58$) is 409 nm and is red-shifted to 480 nm in a more polar ACN/THF mixed solvent ($\epsilon = 24.6$). Solvents of high polarity favor the formation of ion pairs or free ions because of stabilization of the ions by solvation whereas solvents of low polarity favor the formation of an exciplex. It is known that even when the PET is endoergic the formation of an exciplex is possible because of electronic coupling between the locally excited state and the charge transfer (CT) state. If that is the case, then higher generation dendrimers may have lower reduction potential than that of the lower generation dendrimers. We did not attempt to check the redox potentials of these dendrimers as a function of generation.

The nature of the quenching process will be elaborated here. The quenching of fluorescence may occur either through dynamic quenching or static quenching. In dynamic quenching, the fluorophore and the quencher diffuse to form the encounter complex when they are within the distance of closest approach and subsequently electron transfer takes place. In static quenching, a ground-state complex is formed between the fluorophore and quencher which does not emit in the excited state. Such a complex is called a dark complex. Static quenching is inferred from the positive deviation and high value of k_{SV} in the Stern−Volmer plot for the quenching of the steady-state fluorescence intensity. In the dendrimers under study, the quenching of the fluorescence of lower generation dendrimers is exclusively due to dynamic quenching as evidenced by the similarity of the Stern−Volmer quenching constant by steady-state intensity ($K_{SV}(I)$) measurements and lifetime ($K_{SV}(\tau)$) measurements. However, in the higher generations, static quenching also contributes in addition to dynamic quenching as inferred from the high values of $K_{SV}(I)$ for these dendrimers compared to $K_{SV}(\tau)$. The values of $K_{SV}(\tau)$ for **1**, **4**, and **5** are 101.0, 111.5, and 107.6 M^{-1}, respectively. The nearly constant values of $K_{SV}(\tau)$ suggest the lack of dependency of the quenching rate constant on the size of the dendrimer. This result is not surprising when considering the competing effects of size on the diffusion rate. The diffusion-controlled rate constant is given by eq 4:

$$k_{diff} = 4\pi(D_A + D_B)R \tag{4}$$

$$D = kT/6\pi\eta r \tag{5}$$

where k_{diff} is the rate of diffusion, D the diffusion coefficient, R the distance of closest approach which is equal to the sum of the radii of the two reactants A and B ($R = r_A + r_B$), k the Boltzman constant, T the temperature in Kelvin, η the viscosity of the solvent, and r the radius of the reactant. Increasing the size of the reactant will increase the distance of closest approach which will enhance the diffusion rate. At the same time, diffusion will be retarded by the larger reactant as the diffusion coefficient is inversely proportional to the size of the reactants. Thus, the opposing effects may cancel each other. However, caution should be taken in interpreting these results since the higher generation dendrimers are much larger than the quench-

er (DABCO). Normally, in the study of the quenching of the fluorescence of small organic molecules the sizes of the fluorescing species and the quencher are assumed to be identical and the size dependence of the rate constant is ignored.

Even though the high values of $K_{SV}(I)$ in the higher generation dendrimers is attributed to the formation of a ground-state complex (static quenching), the absorption spectra of **5** and **6** with DABCO do not show any spectral shift or broadening with the mM concentrations used for the fluorescence quenching study. With higher concentrations (0.1−0.8 M) of DABCO in THF a small increase in absorbance at longer wavelengths was observed, indicating the formation of a ground-state complex. From the Benesi−Hildebrand plot the formation constant for the complexes was determined to be 3.2 and 4.5 M^{-1} for **5** and **6**, respectively. It is also possible that the negative deviation due to exciplex emission may outweigh the positive deviation due to static quenching in these dendrimers.

As seen from Table 1, the bimolecular quenching rate constants for *p*-DCB and *p*-DMB are almost identical, even though their numerical values of redox potentials differ by 0.3 V with *p*-DCB having the higher value. For the formation of an ion pair from the electron transfer in the excited state, the free energy change (ΔG_{et}) is given by eq 6:

$$\Delta G_{et} = E_D^{1/2} - E_A^{1/2} - E_{0,0} - e^2/d\epsilon \qquad (6)$$

where $E_D^{1/2}$ is the oxidation potential of the donor, $E_A^{1/2}$ is the reduction potential of the acceptor, $E_{0,0}$ the singlet excitation energy of the fluorescing species, e is the electronic charge, d is the distance between the ions, and ϵ is the dielectric constant of the solvent. Even though both quenchings occur at identical rate constants despite the difference in the redox potentials of these two quenchers, it is misleading to draw conclusions about the electron donor/acceptor capability of the dendrimer from the quenching rate constant alone. However, as these quenching rate constants are close to the diffusion-controlled rate constants for ACN, these dendrimers have equally good electron-donor and electron-acceptor properties. Hence, these tolan-based dendrimers are good systems for making model compounds to mimic photosynthesis as they can easily facilitate the charge transport. A detailed study of photoinduced intramolecular electron transfer in dendritic macromolecules with suitable electron acceptor/donor groups is underway in our laboratory. A premilinary report of an anomalous spectral shift observed in the fluorescence of higher generations of these dendrimers has been published elesewhere.[45]

Conclusions

We have shown that effective intermolecular electron transfer is the mechanism by which the fluorescence of the dendrimers **1**−**6** is quenched by various electron acceptors and donors. Hence, these dendrimers under study may act as either electron acceptors or donors, and they are suitable bridging medium for model compounds to mimic photosynthesis. The observation of additional emission in the long-wavelength range suggests that the high-generation dendrimers tend to form exciplexes where as lower generation dendrimers form ion pairs. The additional emission introduces negative deviation in the Stern−Volmer plot for the higher generation dendrimers. In the case of higher generation dendrimers, there is substantial contribution from static quenching, but in lower generation dendrimers the process is exclusively due to dynamic quenching. Formation of ground-state complexes has been observed for the higher generation dendrimers **5** and **6** with DABCO. The size of the dendrimer has little effect on the dynamic quenching of the fluorescence. This study indicates that it is feasible to effect photoinduced intramolecular electron transfer in these dendritic macromolecules with a suitable choice of electron donor/acceptor functionality at the core.

Acknowledgment. This work was supported by the National Science Foundation, Grant DMR 95-20402. Additional support from Du Pont, the Alfred P. Sloan Foundation, and the Camille Dreyfus Teacher−Scholar Awards Program is gratefully acknowledged.

References and Notes

(1) Kirmaier, C.; Holten, D. *Photosynth. Res.* **1987**, *13*, 225.
(2) Timpe, H.-J. *Top. Curr. Chem.* **1990**, *156*, 167.
(3) Hageman, H. J. In *Photopolymerization and Photoimaging Science and Technology*; Allen, N. S., Eds.; Elsevier Applied Science: London, 1989.
(4) Fouassier, J.-P. In *Photoinitiation, Photopolymerization, and Photocuring: Fundamentals and Applications*; Hanser Publishers: Munich, 1995.
(5) Crivello, J. V. *Adv. Polym. Sci.* **1984**, *62*, 1.
(6) *Radiation Curing in Polymer Science and Technology-Volume II*; Fouassier, J. P., Rabek, J. F., Eds.; Elsevier Applied Science: London, 1993.
(7) Sahyun, M. R. V. *Chemtech* **1992**, 418.
(8) Hamilton, J. F. In *Handbook of Imaging Materials*; Diamond, A. S., Ed.; Marcel Dekker: New York, 1991.
(9) Eaton, D. F. *Top. Curr. Chem.* **1990**, *156*, 199.
(10) Borsenberger, P. M.; Weiss. D. In *Organic Photoreceptors for Imaging Systems*; Marcel Dekker: New York, 1993.
(11) Law, K.-Y. *Chem. Rev.* **1993**, *93*, 449.
(12) Wiederrecht, G. P.; Yoon, B. A.; Wasielewski, M. R. *Science* **1995**, *270*, 1794.
(13) Tamura, K.; Padias, A. B.; Hall, Jr., H. K.; Peyghambarian, N *Appl. Phys. Lett.* **1992**, *60*, 1803.
(14) Fox, M. A. *Chemtech* **1992**, 680.
(15) Rajeshwar, K. *Chem. Ind. (London)* **1996**, 454.
(16) Gratzel, M. *Chimia* **1996**, *50*, 583.
(17) Frei, H.; Blatter, F.; Sun, H. *Chemtech* **1996**, 24.
(18) Natansohn, A. *Polym. Adv. Tech.* **1994**, *5*, 133.
(19) Baumgarten, M.; Müllen, K. *Top. Curr. Chem.* **1994**, *169*, 1.
(20) Marcus, R. A. *J. Chem. Phys.* **1956**, *24*, 966.
(21) Marcus, R. A.; Sutin, N. *Biochim. Biophys. Acta* **1985**, *811*, 265.
(22) Rehm, D.; Weller, A. *Isr. J. Chem.* **1970**, *8*, 259.
(23) Kavarnos, G. J. In *Fundamentals of Photoinduced Electron Transfer;* VCH Publishers: New York, 1993.
(24) Fox, M. A.; Chanon, C. *Photoinduced Electron-Transfer Parts A, B, C & D*; Elsevier: Amsterdam, 1988.
(25) Tomalia, D. A.; Durst, H. D. *Top. Curr. Chem.* **1993**, *165*, 194.
(26) Newkome, G. R.; Moorefield, C. N. *Aldrichim. Acta* **1992**, *25*, 31.
(27) Frèchet, J. M. J. *Science* **1994**, *263*, 1710.
(28) Xu, Z.; Kyan, B.; Moore, J. S. In *Advances in Dendritic Macromolecules*; Newkome, G. R., Ed.; Jai Press: Greenwich, 1994; Vol. 1.
(29) Wang, P.-W.; Liu. Y−J.; Devadoss, C.; Bharathi, P.; Moore, J. S. *Adv. Mater.* **1996**, *8*, 237.
(30) Devadoss, C.; Bharathi, P.; Moore, J. S. *J. Am. Chem. Soc.* **1996**, *118*, 9635.
(31) Moreno-Bondi, M. C.; Orellana, G.; Turro, N. J.; Tomalia, D. A. *Macromolecules* **1990**, *23*, 910.
(32) Janssen, R. A. J.; Jansen, J. F. G. A.; van Haare, J. A. E. H.; Meijer, E. W. *Adv. Mater.* **1996**, *8*, 494.
(33) Sadamoto, R.; Tomioka, N.; Aida, T. *J. Am. Chem. Soc.* **1996**, *118*, 3978.
(34) Kimura, M.; Nakada, K.; Yamaguchi, Y.; Hanabusa, K.; Shirai, H.; Kobayashi, N. *Chem. Commun.* **1997**, 1215.
(35) Dumas, J. N.; Crosby, J. A. *J. Phys. Chem.* **1971**, *75*, 991.

(36) Chakravorty, S. C.; Ganguly, S. C. *Z. Phys. Chem. (Neue Folge)* **1970**, *72*, 34.
(37) Tanzaki, Y.; Inoue, H.; Hoshi, T.; Shirashi, J. *Z. Phys. Chem. (Neue Folge)* **1971**, *74*, 45.
(38) Mattes, S. L.; Farid, S. *J. Chem. Soc., Chem. Comm.* **1980**, 457.
(39) Horner, L.; Dickerhof, K. *Chem. Ber.* **1983**, *116*, 1615.
(40) Beens, H.; Weller, A. In *Organic Molecular Photophysics*; Birks, J. B., Ed.; Wiley: New York, 1975; Vol. 2.
(41) Caldwell, R. A.; Creed, D. *Acc. Chem. Res.* **1980**, *13*, 45.
(42) Mattes, S. L.; Farid, S. *Science* **1984**, *226*, 917.
(43) Gould, I. R.; Young, R. H.; Mueller, L. J.; Farid, S. *J. Am. Chem. Soc.* **1994**, *116*, 8176.
(44) Kuzmin, M. G. *J. Photochem. Photobiol. A: Chem.* **1996**, *102*, 51.
(45) Devadoss, C.; Bharathi, P.; Moore, J. S. *Angew. Chem., Int. Ed. Engl.* **1997**, *36*, 1633.
(46) Murov, S. L.; Carmichael, I.; Hug, G. L. *Handbook of Photochemistry*, 2nd ed.; Marcell Dekker: New York, 1993.

MA980225I